Macromolecular Research Article

DOI 10.1007/s13233-019-7084-6 www.springer.com/13233 pISSN 1598-5032 eISSN 2092-7673

Synthesis and Antibacterial Activities of Boronic Acid-Based Recyclable Spherical Polymer Brushes

Hüseyin Cicek*[,1]
Gökhan Kocak[2]
Özgür Ceylan[3]
Vural Bütün[4]

[1] Department of Chemistry, Muğla Sitki Koçman University, Muğla, 48000, Turkey
[2] Department of Chemistry, Adiyaman University, Adiyaman, 02040, Turkey
[3] Food Quality Control and Analysis Program, Ula Ali Kocman Vocational School, Muğla Sitki Koçman University, Muğla, Ula, 48147, Turkey
[4] Department of Chemistry, Eskisehir Osmangazi University, Eskisehir, 26480, Turkey

Received May 1, 2018 / Revised October 3, 2018 / Accepted November 19, 2018

Abstract: Crosslinked poly(4-vinylbenzyl chloride) (PVBC) microbead was prepared by suspension polymerization. Various spherical polymer brushes (SPBs) were produced by grafting polymeric chains on their surfaces *via* surface initiated-atom transfer radical polymerization (SI-ATRP) using 4-vinylphenyl boronic acid (VPBA), 2-(dimethylamino)ethyl methacrylate (DMA), and quaternized DMA (QDMA). PVBC-*g*-PDMA, PVBC-*g*-PQDMA, PVBC-*g*-PVPBA, PVBC-*g*-P(VPBA-*b*-DMA), PVBC-*g*-P(VPBA-*co*-DMA) and PVBC-*g*-P(VPBA-*b*-QDMA) SPBs were characterized using nuclear magnetic resonance spectroscopy, attenuated total reflection Fourier transform infrared spectroscopy, thermogravimetric analysis, and scanning electron microscopy. Antibacterial activities of the synthesized SPBs were investigated against *Escherichia coli* and *Staphylococcus aureus* in nutrient and nutrient free media. Although PVBC-*g*-P(VPBA-*b*-DMA) SPB provided high antibacterial activity in the nutrient containing media due to its antibacterial, anti-biofilm and anti-QS properties, PVBC-*g*-P8QDMA SPB was found to be more effective in nutrient free media. Considering repeatable antibacterial activity, the PVBC-*g*-P(VPBA-*b*-8QDMA) SPB has advantageous over PVBC-*g*-P(VPBA-*b*-DMA) and PVBC-*g*-P8QDMA SPBs for long-term applications such as wastewater treatment in fluidized bad system.

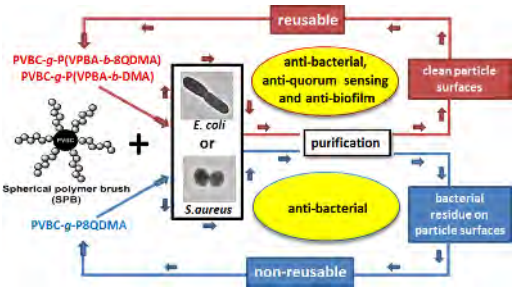

Keywords: antibacterial microbead, suspension polymerization, SI-ATRP, spherical polymer brushes, 4-vinylbenzyl chloride, 4-vinylphenyl boronic acid, 2-(dimethylamino)ethyl methacrylate.

1. Introduction

Antibacterial solid surfaces are being used in hospital, dental equipments,[1] water purification,[2,3] food preservation,[4] textiles,[5] wood,[6] paper,[7,8] shoes,[9] and many other places to reduce the risks of microbial infections. Killing (active) and prevention (passive) are main methods to inhibit bacterial population with antibacterial surfaces.[10] There is a direct interaction between the antibacterial surface and bacteria in killing mechanism. On the other hand, prevention involves steric and/or electrostatic repulsion, low surface energy and anti-quorum sensing (anti-QS) properties of surface that prevent the increase in bacteria population.

Among the solid surfaces and drug delivery systems,[11] polymer beads (PBs) owns a special place in antibacterial applications. They have surface modification capabilities as they can have different functionalities using surface initiated-atom transfer radical polymerization (SI-ATRP) and surface-initiated reversible addition-fragmentation chain-transfer (SI-RAFT) polymerization, hydrolysis and condensation reactions and grafting techniques to obtain the antibacterial beads.[3,5-7,12-15] Most popular preferred techniques for surface polymerization are controlled living radical polymerizations such as ATRP. As an example, SI-ATRP has particular advantages. It requires less stringent experimental conditions and has great tolerance for various functional monomers. It also provides a strong bond between the substrate and polymer chains on the surface, well-controlled chain length and compositions with a great number of architectures. Its successful applications for the preparation of well-defined polymer brushes on different substrates, such as silicon, silica, gold, polymers have been well reported by various research groups.[16,17] Micro-PBs are easily recoverable and reusable. Suspension polymerization has been used to produce antibacterial PBs of sized between 10 and 1000 μm size having various functional groups on their surfaces such as amine, carboxyl, hydroxyl, glycidyl and halogens.[18-25]

Polymeric form of 2-(dimethylamino)ethyl methacrylate (DMA) and its quaternized forms (QDMA) are well-known for their high antibacterial activities.[2,26-28] There are several reports and reviews published on the antibacterial effectiveness of the stated polymer and similar polymeric structures.[15,29,30] Boron has great physical and chemical properties which offer an opportunity to discover new pioneering drug discovery areas. Boron therapeutics reveal different modes of inhibition against different biological targets.[31] Antibacterial SPBs of nearly 250 μm diameter have been produced by the quaternization of PDMA (PQDMA) brushes on

Acknowledgments: The authors would like to express their thanks to the Scientific and Technological Research Council of Turkey (TUBITAK, grand no. 213M181) for financial support.

***Corresponding Author:** Hüseyin Cicek (hcicek@mu.edu.tr)

their surfaces using SI-ATRP tecniques.[2] The polymer produced from the 4-vinylphenyl boronic acid (VPBA), a boron containing monomer, has been used in various boronic acid affinity studies.[23,32-37] They are also prone to show antibiofilm properties as they boronic acids show anti-QS activities.[38,39] In the literature, there are a great number of reports on the antibacterial activity of boron based compounds, but studies on the antibacterial activity of boron-containing polymers are very limited. In our previous study, we have reported antimicrobial and anti-quorum sensing activities of dyes containing new diazaborine and phenylboronic acid based copolymer.[40,41] As far as we know from literature, this study is a pioneering study that demonstrates the antibacterial effect of boron-based recycled polymeric microbeads.

This study was aimed to obtain antibacterial spherical polymer brushes (SPBs) carrying both killing and preventive properties. PVBC microbeads carrying DMA and VPBA copolymeric brushes were synthesized by SI-ATRP. DMA residues on blocks were quaternized to provide antibacterial activities to the particles. The synthesized PBs can be recycled as antibacterial inhibitors.

2. Experimental

2.1. Materials

4-Vinylbenzyl chloride (VBC, 90.0%, Milwaukee, WI, USA), VPBA (Aldrich), ethylene glycol dimethacrylate (EGDMA, Aldrich, 98.0%), 2-(dimethylamino)ethyl methacrylate (DMA, Aldrich, 98.0%), 2,2′-azobis(2-methylpropionitrile) (AIBN, 98.0%, SIAL, St. Louis, MO, USA), 2,2′-bipyridyl (Bpy, Alfa Aesar, 99.0%), CuBr (Aldrich, 99.9%), methyl iodide (SIAL, 99.0%), pentyl iodide (Aldrich, 98.0%), octyl iodide (Aldrich, 98.0%,), dimethylformamide (DMF, Merck, 99.8%), chloroform ($CHCl_3$, SIAL, 99.0%), dichloromethane (CH_2Cl_2, SIAL, 99.8%), tetrahydrofuran (THF, SIAL, 99.9%), ethanol (EtOH, SIAL, 99.8%), anhydrous diethyl ether (SIAL, 99.5%), poly(vinyl alcohol) (PVA, g mol^{-1}, average M_w=85,000-124,000, 87.0-89.0% hydrolyzed, Aldrich), methanol (MeOH, 99.0%, Merck, Darmstadt, Germany), and ethylenediaminetetraacetic acid (EDTA, SIAL, 98.5%) were bought from the stated commercial sources. All monomers were passed through a silica gel or basic alumina column prior to polymerization to remove the inhibitor.

2.2. Instruments and measurements

Scanning electron microscope (SEM) images of samples was captured by Jeol JSM-7600F (Tokyo, Japan) to determine the antibiofilm properties of bacteria, yeast and dyes that contained copolymers. Samples were Au/Pd coated to provide conductivity. Approx. 100 particles were counted on SEM photographs to determine the number average diameter (D_n) with Eq. (1).

$$D_n = \sum N_i D_i / \sum N_i \quad (1)$$

where N_i is the number of particles of diameter D_i (μm).

Thermogravimetric analysis (TGA) of all microbeads with increasing temperature were obtained by TGA 400 (Perkin Elmer, Waltham, MA, USA) with 10.0 °C min^{-1} heating rate under N_2 (g) atmosphere. Attenuate total reflection-Fourier transform infrared (ATR-FTIR) measurements were carried out using Perkin Elmer Spectrum 100 spectrometer (Perkin Elmer, Waltham, MA, USA). The pictures of microbeads and spherical polymer brushes (SPBs) were determined with E100 optical microscope (Nikon, Tokyo, Japan). Boron-11 NMR experiments were conducted using a JEOL ECZ500R (JEOL Co., Tokyo, Japan) NMR spectrometer.

2.3. Preparation of PVBC microbeads and their derivatization with polymeric brushes

The crosslinked PVBC microbeads were prepared by suspension polymerization (Figure 1(a)).[42] VBC (8.0 mL, 51.1 mmol), EGDMA (2.4 mL, 12.5 mmol), and AIBN (35.0 mg, 0.2 mmol) were dissolved in toluene (12.0 mL). The reaction mixture was purged with nitrogen (15 min) to remove oxygen and dispersed in an aqueous medium, prepared by dissolution of PVA (0.4 g) in water (130.0 mL). Polymerization was carried out in a magnetically stirred (1000 rpm) 2-neck round bottom flask equipped with a reflux condenser and sealed with rubber septum (250.0 mL) at 78 °C for 24 h. The prepared PVBC microbeads were washed exhaustively (water 2 h, EtOH and THF) to remove the unwanted moieties and dried in vacuo at room temperature for two days. Six different SPBs were prepared using SI-ATRP technique[2,3,6,26,28,42,43] by changing the sequence of the monomers added to the polymerization environment (See Table S1 for reagents used).

To obtain PDMA on PVBC microbeads by SI-ATRP, PVBC microbeads (2.0 g) were first added into a magnetically stirring (400 rpm) reaction mixture in a glass flask (50.0 mL) containing DMA (8.0 mL, 46.5 mmol), Bpy (0.37 g, 0.23 mmol), CuBr (0.16 g, 0.11 mmol) and DMF (5.0 mL). Nitrogen was flushed for 20 min to remove the dissolved oxygen. The flask was sealed, polymerization was carried out at 65 °C for 48 h. After the reaction was terminated, the SPBs were washed several times with a 10% EDTA solution for 24 h to remove copper. Finally, all SPBs were subjected to exhaustive washing with THF, 0.01 M HCl, water and MeOH. PVBC-*g*-PDMA (Type A) SPB was obtained after drying in vacuo at room temperature for 48 h. PVBC-*g*-PVPBA (Type C) SPB was obtained similarly, except VPBA was used instead of DMA monomer (See Table S1 for reagents used).

A typical modified procedure for the synthesis of PVBC-*g*-P(VPBA-*b*-DMA) SPB (Type E) is as follows: PVBC microbeads (2.0 g) were added into a reaction mixture containing VPBA (0.2 g, 1.35 mmol), Bpy (0.37 g, 0.23 mmol), CuBr (0.16 g, 0.11 mmol) and DMF (5.0 mL). The reaction mixture was purged with nitrogen for 20 min to remove the dissolved oxygen. The flask was sealed and polymerization was carried out at 65 °C for 28 h while the mixture stirred at 400 rpm. DMA (8.0 mL, 46.5 mmol) was added to the reaction medium under nitrogen bridge, allowed to proceed for further 24 h. PVBC-*g*-P(VPBA-*b*-DMA) SPB (Type E) was obtained after washing (same as the one used to wash homopolymer spherical brushes). SPB carrying random brushes (Type D) have been synthesized by reacting the two monomers simultaneously.

The Type A and Type E SPBs containing PDMA were quaternized with methyl iodide, pentyl iodide and octyl iodide (Figure 1(b)). It was desired to check the change in the antibacterial

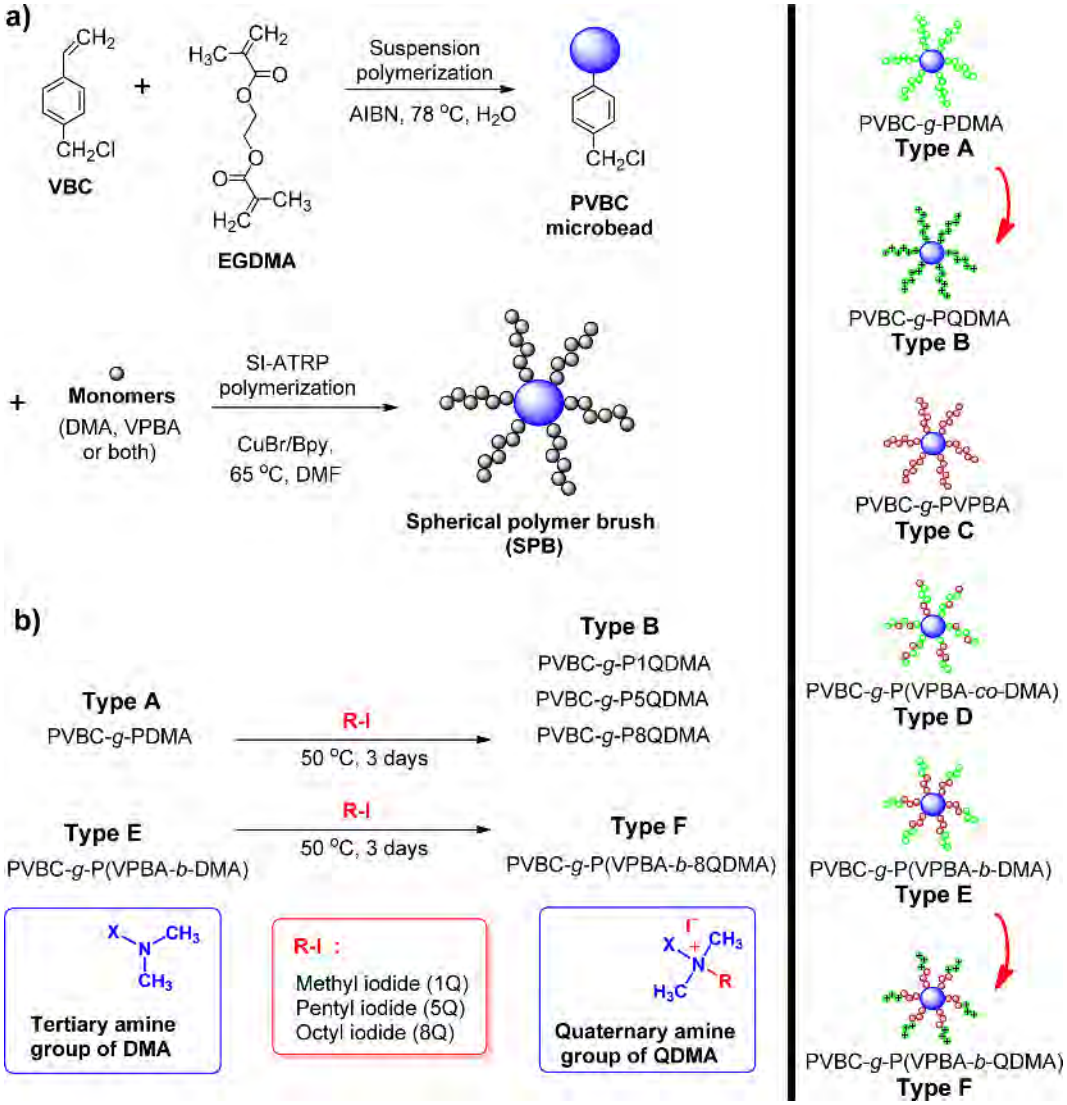

Figure 1. Synthetic pathway of microbeads and SPBs.

activity of the beads having alkyls of various lengths. Quaternization of the polymer brushes containing DMA (QDMA) was carried out by stirring these SPBs (2.0 g) with excess of alkyl iodides (5.0 mL) at 50 °C for 72 h under a nitrogen atmosphere in a 50.0 mL glass flask.[7,27,44] After exhaustively washed with THF and MeOH, the synthesized quaternized SPBs were dried *in vacuo* at room temperature for 72 h (See Table S2 for codes of quaternized spherical brushes).

2.4. Antibacterial activity

Antibacterial activity of the microbeads was performed according to the literature,[2] in phosphate buffer saline (PBS); with and without nutrient.

Two different antibacterial tests were performed with nutrient-containing PBS. First, the aim was to determine the amount of SPBs needed to completely inhibit 8.0×10^5 colony forming unit per milliliter (CFU/mL) initial bacteria population after 24 h incubation. For this, *Escherichia coli* ATCC 25922 (American type culture collection, Mananas, VA, USA) and *Staphylococcus aureus* ATCC 25923 (American type culture collection, Mananas, VA, USA) were separately cultivated in 50.0 mL of a 3.1% yeast-dextrose broth. Dry SPBs were added into this inocula to get the final SPBs concentrations ranging from 8.0-32.0 mg/mL for *E. coli* and 1.0-4.0 mg/mL for *S. aureus*. Incubation temperature was kept constant at 30 °C and 35 °C for *E. coli* and *S. aureus*, respectively. The SBP concentration, at which all bacteria in the medium were inhibited, was determined as the minimum inhibition concentration (MIC) of SBP.

Another target was to follow antibacterial reduction with time in nutrient containing media. *E. coli* or *S. aureus* was cultivated in 50.0 mL containing 3.1% yeast-dextrose broth with initial bacterial concentration of 4.0×10^7 CFU/mL. 30 mg of SPBs were added to 20.0 mL of the stated medium to obtain 1.5 mg/mL of final SPB concentration. The mixtures were incubated at 200 rpm and 37 °C. Absorbance of the medium was kinetically recorded on a UV-visible spectrophotometer at 600 nm to follow bacteria multiplication.

In antibacterial tests with nutrient-free PBS, *E. coli* was cultivated in 50.0 mL of a 3.1% yeast-dextrose broth (containing

10.0 g/L peptone, 8.0 g/L beef extract, 5.0 g/L sodium chloride, 5.0 g/L glucose, and 3.0 g/L yeast extract of pH 6.8) at 37 °C. The *E. coli* cells were centrifuged at 5,000 rpm for 10 min. The precipitated cells were washed twice with a sterile PBS and resuspended in nutrient-free PBS to obtain an initial cell concentration of 1×10^6 CFU/mL. 30 mg of SPBs were added into 20.0 mL of the stated PBS suspension and incubated at 200 rpm and 37 °C. The viable *E. coli* cells were counted by using surface spread-plate method. In this method, first 1.0 mL of bacteria culture was taken at predetermined time intervals to prepare serial dilutions with PBS. 0.1 mL of the diluted sample from each serial dilution was then spread onto solid growth agar plate. The numbers of viable colonies were counted manually; real number was calculated as 1×10^6 CFU/mL by considering the dilution factor. The same method used for *E. coli* was applied for *S. aureus* antibacterial activity determination. Two times tested microbeads were used in antibacterial experiments. The particles were sonicated three times (before the tests) in EtOH/THF (1:1, v/v) and allowed to stand for 10 min under UV. SPBs were imaged with SEM after the surfaces were coated with gold before and after purification.

3. Results and discussion

3.1. Characterization of PVBC microbeads and SPBs

Using Eq. (1), SEM photographs provided the average size of PVBC microbeads (Figure 2(a)) as 241.9 ± 51.8 μm. Figure 2 shows the modified surface of PVBC microbeads. The widest pore on PVBC microbeads surface (Figure 2(a)) is approximately 50 nm. The pores get closed and aggregates formed when the PVPBA brushes were added onto it (Figure 2(b)). The complete disappearance of the pores on the surface of the PVPBA brushes by the addition of the PDMA blocks can be considered a sign of successful surface modification. Pits were formed on the surface of PVBC-*g*-P(VPBA-*b*-DMA) SPB (Figure 2(c)) due to the impact of the magnetic stirrer on the particle surface after long stirring. In spite of these pits, microbeads could be used in antibacterial tests because they did not lose their integrity.

The ATR-FTIR spectra of the PVBC microbeads, PVBC-*g*-PVPBA, PVBC-*g*-PDMA, and PVBC-*g*-P(VPBA-*b*-DMA) SPBs are presented in Figure 3. The absorption bands were observed at 668 (stretch C-Cl), 1728 (stretch C=O, ester), 1614 (stretch C=C, phenyl ring), and 2820-2925 cm^{-1} (stretch C-H). Stretching B-O band around 1350 cm^{-1} related to -$B(OH)_2$ supports the successful grafting of VPBA on the PVBC.[45,46] There is no significant difference between other peaks (Figure 3(a) and (b)) as the structures of VBC and VPBA monomers are similar, as well as due to very low proportion of VPBA in the copolymer structure. Amine groups on PDMA provided a weak peak around 1600 cm^{-1} (stretch C-N) after modification (Figure 3(c)). The sharpness of this peak decreased as the amount of PVPBA increased as block polymer before PDMA block on the PVBC microbeads (Figure 3(d)).

The presence of PVPBA segments at the particle surface can

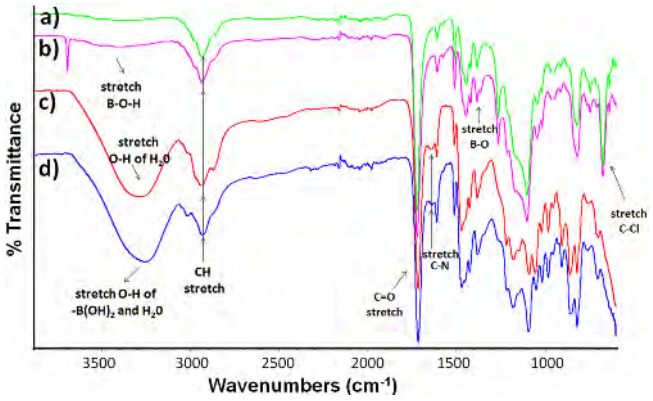

Figure 3. ATR-FTIR spectra of; (a) PVBC microbeads, (b) PVBC-*g*-PVPBA, (c) PVBC-*g*-PDMA, and (d) PVBC-*g*-P(VPBA-*b*-DMA) SPBs.

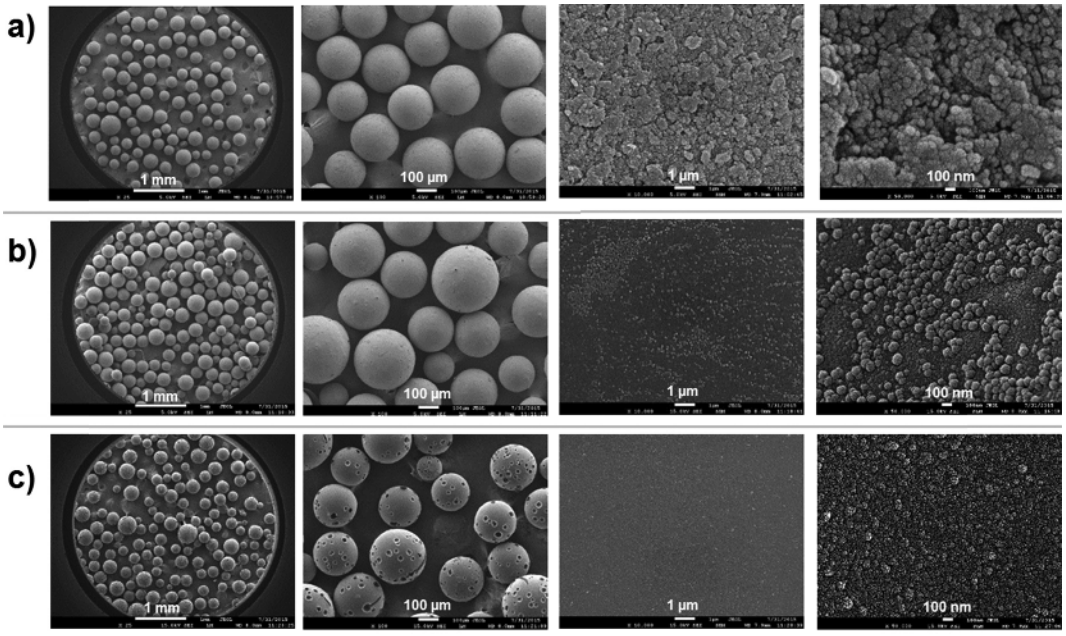

Figure 2. SEM images of microbeads at different magnifications (from left to right 25×, 100×, 10000×, and 50000×); (a) PVBC microbead, (b) PVBC-*g*-PVPBA, and (c) PVBC-*g*-P(VPBA-*b*-DMA) SPBs.

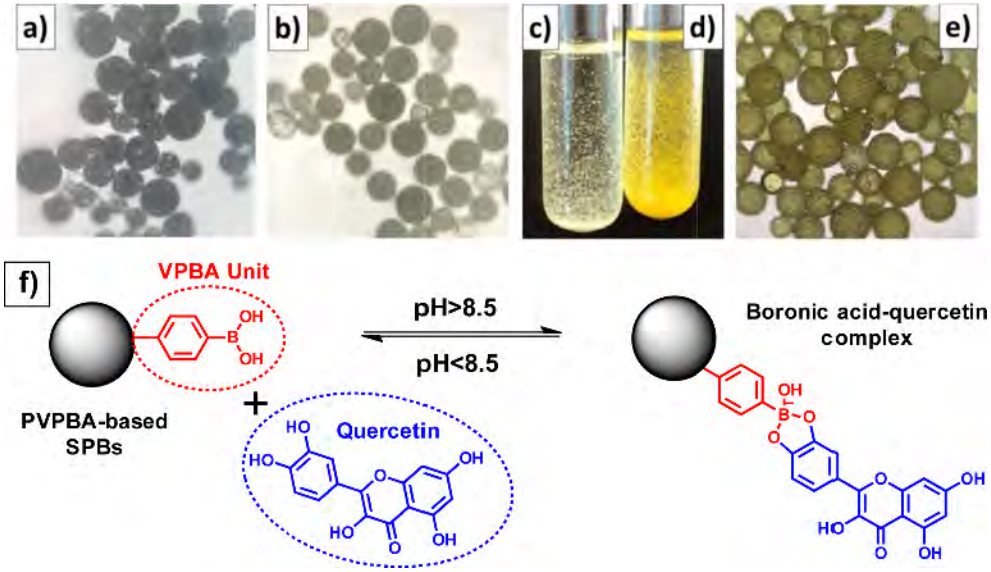

Figure 4. Optical microscope photograph of PVBC microbeads; (a) before treatment with quercetin, (b) PVBC-*g*-PVPBA SPB before treatment with quercetin, (c) PVBC beads after treatment with quercetin, (d) PVBC-*g*-PVPBA SPB after treatment with quercetin, (e) PVBC-*g*-PVPBA SPB after treatment with quercetin (bar:1 mm =25 μm), and (f) complex formation of PVPBA-based SPBs and quercetin (1,2-diol) in aqueous solution.

be observed on naked eye by the reaction of phenyl boronic acid with 1,2-diols (Figure 4(f)). For this purpose, quercetin (as a model 1,2-diol) was interacted with PVBC-*g*-PVPBA SPB at pH 8.5.[47] Digital photographs of the particles, before and after interaction with quercetin, are presented in Figure 4. The gray color of the PVBC beads (Figure 4(a)) did not change after the interaction with quercetin (Figure 4(c), left tube), but PVBC-*g*-PVPBA beads (Figure 4(b)) turned into yellow when interacted with quercetin (Figure 4(d) and (e)). This yellow color indicates that quercetin has been captured by the boron atoms present on the surface of PVBC-*g*-PVPBA.

ATR-FTIR spectra of PVBC-*g*-PDMA and its quaternized forms with different alkyl lengths are given in Figure S1(a)-(c). Quaternization increased the intensity of C-H stretch peak around 2820-2925 cm^{-1} depends on the length of alkyl chain. FTIR spectra of PVBC with random or block copolymeric brushes of PVPBA, PDMA and P8QDMA are presented in Figure S2. Although there is no significant difference between block and random polymeric forms of VPBA and DMA (Figure S2(b) and (c)), the effect of alkyl length is clearly visible (Figure S2(a)) in the form of band intensity of CH_2 around 2820-2925 cm^{-1}. The peak appeared at 3200-3600 cm^{-1} in case of SPBs is -OH stretching vibration of H_2O (Figure S2(b) and (c)).

The broad signal in the range 0-40 ppm observed in ^{11}B solid-state NMR spectrum of PVBC-*g*-P(VPBA-*co*-DMA) SPB (Figure S3) shows the presence of boronic acid in the structure of SPB. In the ^{11}B NMR spectrum of PVBC-*g*-P(VPBA-*b*-DMA) SPB, the PVPBA block could not be observed in the structure because it remained in the interior.

The TGA curves of PVBC microbeads and its modified forms are presented in Figure 5. PVPBA arms on PVBC-*g*-PVPBA SPB decreased the thermal degradation temperature of PVBC microbeads.[48-50] PVBC-*g*-PDMA SPB showed lower maximum rate of the degradation temperature (the first step at T_{max}~150 °C) with three steps. TGA results we obtained with the thermal decomposition

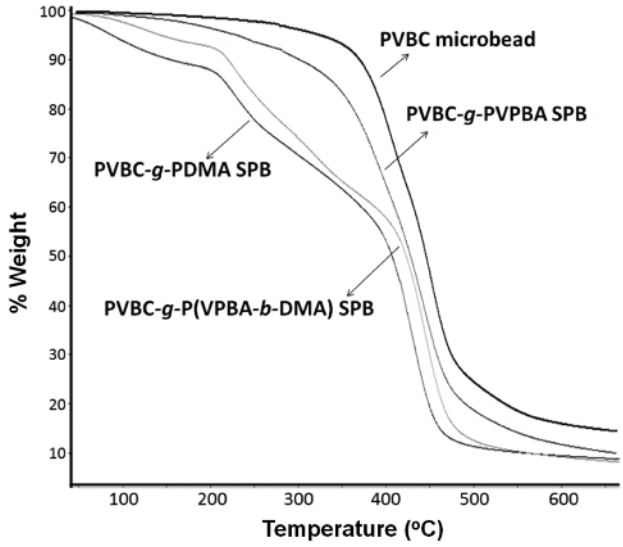

Figure 5. TGA curves of PVBC, PVBC-*g*-PVPBA, PVBC-*g*-PDMA, and PVBC-*g*-P(VPBA-*b*-DMA) SPBs.

behavior of the PDMA homopolymer (the first step at ~167 °C, the second step at ~306 °C and the third step at ~403 °C) is quite similar with the data given in the literature.[7,51] On the other hand, the PVPBA homopolymer is degraded in one step and the decomposition temperature (T_{max}) is determined as 451 °C in the previous study.[52] As reported in the literature, PVPBA is more thermally resistant than PDMA.[7,51,52] The thermal degradation of PDMA-containing SPBs showed large mass decreases at ~300 and ~450 °C, while the thermal decomposition temperature of PVBC and PVBC-*g*-PVPBA microspheres was determined at higher temperatures (T_{max} 430-450 °C).

3.2. Antibacterial activity

Antibacterial activities of the modified PVBC microbeads in nutri-

Table 1. Antibacterial activities of SPBs against *S. aureus* and *E. coli*

Code	Chemical structure of microbead and SPBs	Bead concentration (mg/mL) for 100% inhibition	
		S. aureus	*E. coli*
PVBC	PVBC	>4	>32
Type A	PVBC-*g*-PDMA	<1	16-32
Type B1	PVBC-*g*-P1QDMA	<1	16-32
Type B2	PVBC-*g*-P5QDMA	2-4	16-32
Type B3	PVBC-*g*-P8QDMA	<1	16-32
Type C	PVBC-*g*-PVPBA	>4	>32
Type D	PVBC-*g*-P(VPBA-*co*-DMA)	1-2	16-32
Type E	PVBC-*g*-P(VPBA-*b*-DMA)	<1	8-16
Type F	PVBC-*g*-P(VPBA-*b*-8QDMA)	>4	16-32

ent-containing PBS are presented in Table 1. Smaller particle concentration for 100% inhibition in nutrient-containing PBS means higher antibacterial activity. Particle concentration larger than 4.0 and 32.0 mg/mL for *S. aureus* and *E. coli,* respectively, were not tested since they are insignificant as reported earlier.[2]

Table 1 reflects that PVBC microbeads and PVBC-*g*-PVPBA SPB did not show considerable antibacterial activity as was expected. On the other hand, PVBC-*g*-PDMA, PVBC-*g*-P1QDMA, and PVBC-*g*-P8QDMA required lower SPB concentration for inhibit 100% of bacteria, which means they have higher antibacterial activities. Literature shows that when PDMA is quaternized with longer alkyl chains (8-12 carbons), it reflects higher antibacterial activity.[2,26-29,53] Although increase in alkyl length in the quaternization of PVBC-*g*-PDMA SPB caused approximately similar antibacterial activity against both bacteria, PVBC-*g*-P5QDMA SPB presented less antibacterial activity against *S. aureus* with higher SPB concentration (4.0 mg/mL).

A suitable ratio of hydrophobicity/polarity and solubility are needed to obtain the highest antibacterial activity against *S. aureus*. Since polarity and solubility in aqueous solvents decreases with increasing alkyl group, negative effects may be more than positive if the hydrophobicity of PVBC-*g*-P5QDMA SPB increased. Penetration of polymeric arms into the cell wall of the *S. aureus* with the suitable balance between those effects is needed to gain higher antibacterial activity. While the changes in alkyl group length of PVBC-*g*-P5QDMA SPB did not change inhibition performance of *E. coli*, this changes found to be effective on inhibition *S. aureus*.

Antibacterial activities of PVBC microbeads carrying DMA and VPBA copolymeric brushes were varied in random and block configurations of the monomers in the brushes. PVBC-*g*-P(VPBA-*b*-DMA) SPB provided substantially high antibacterial activity against both bacteria as compared to PVBC and PVBC-*g*-PDMA SPB (Table 1). Random distribution of VPBA and DMA residues in PVBC-*g*-P(VPBA-*co*-DMA) SPB reduced antibacterial activity as compared to PVBC-*g*-PDMA SPB as VPBA residue in random copolymer is less active against bacteria as compared with DMA.[41] On the other hand, PVBC-*g*-P(VPBA-*b*-DMA) has higher antibacterial activity than PVBC-*g*-PDMA.

Detachment of inhibited bacteria from SPBs surface is also very important for sustainability of antibacterial activity. Since adhesion of inhibited bacteria cause covering of the active surface of SPBs and decreased the active antibacterial surface, it is not possible to sustain antibacterial activity with same inhibition rate for longer. The anti-biofilm and anti-QS properties of the PVPBA and PDMA blocks the PVBC-*g*-P(VPBA-*b*-DMA) SPBs, may cause higher antibacterial activity in nutrient containing PBS.[41]

As discussed, the higher anticipated antibacterial activity should be provided by PVBC-*g*-P(VPBA-*b*-8QDMA), which includes both quaternization and VPBA. However, it showed less activity against *S. aureus* as compared to the PVBC-*g*-P8QDMA and PVBC-*g*-P(VPBA-*b*-DMA). This result may be due to two proposed effects: either, PVBC-*g*-P(VPBA-*b*-8QDMA) SPB does not have anti-QS, thus, bacteria can multiply in the presence of nutrient; or P8QDMA segments where bacteria interacts are blocked by PVPBA segments, which are anti-biofilm regions close to the particle surface.[41]

To further clarify the situation, additional antibacterial kinetic studies were performed in nutrient-free PBS with the selected particles (Figure 6) *i.e.* PVBC-*g*-P(VPBA-*b*-DMA) while PVBC-*g*-P8QDMA SPBs were chosen for comparison and PVBC-*g*-P(VPBA-*b*-8QDMA) SPB to explain the unexpected weak antibacterial activity of *S. aureus* in nutrient containing PBS those are expected to exhibit high antibacterial activity.

As Figure 6(a) and (b) shows, bacterial growth reduction capability of particles were observed in the order of PVBC-*g*-P8QDMA>PVBC-*g*-P(VPBA-*b*-8QDMA)>PVBC-*g*-P(VPBA-*b*-DMA) for *E. coli and S. aureus*. PVBC-*g*-P8QDMA particles were able to kill all 1.0×10^6 CFU/mL initial *E. coli* population in almost 5 min; even faster than reported for the same moiety[2] while other particles performed this task in 15 min.

For *S. aureus*, the time for 100% inhibition of 1×10^6 CFU/mL initial bacteria with PVBC-*g*-P8QDMA and PVBC-*g*-P(VPBA-*b*-8QDMA) SPBs are 5 and 15 min, respectively (Figure 6(b)). However, PVBC-*g*-P(VPBA-*b*-DMA) SPB was able to kill 99.0% initial bacteria concentration in 60 min. These results are inconsistent as compared to the ones obtained from the nutrient-containing PBS (Table 1). PVBC-*g*-P(VPBA-*b*-DMA) SPB showed better antibacterial activity in nutrient-containing PBS when compared to PVBC-*g*-P8QDMA and PVBC-*g*-P(VPBA-*b*-8QDMA) SPBs.

To solve this contradiction, antibacterial kinetic studies were performed under high initial bacteria population 4.0×10^7 CFU/mL in nutrient-containing PBS (Figure 7). The growth of *E. coli* in the nutrient-containing PBS slowed down more effectively by PVBC-*g*-P(VPBA-*b*-DMA) SPB than PVBC-*g*-P8QDMA and PVBC-*g*-P(VPBA-*b*-8QDMA) SPB (Figure 7(a)) probably due to the anti-

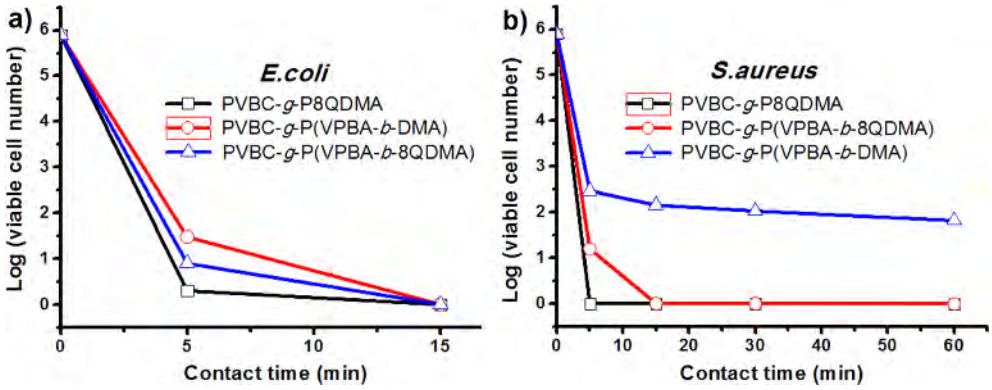

Figure 6. Antibacterial reduction capability of the selected particles for *E. coli* and *S. aureus* at initial bacteria population of 1.0×10^6 CFU/mL.

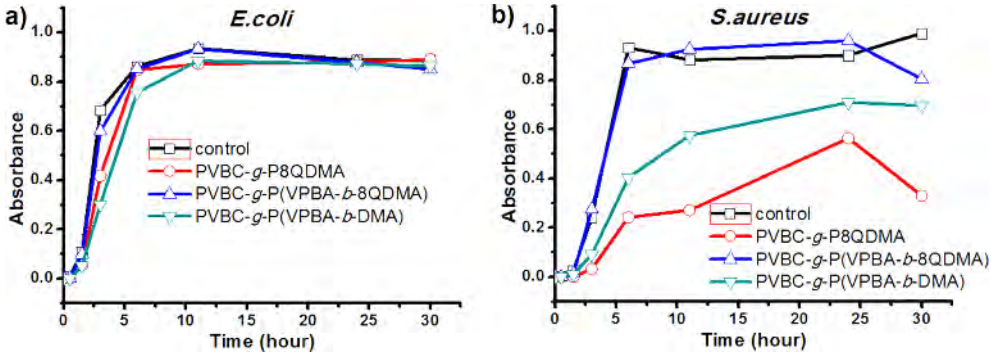

Figure 7. Growth kinetics of *E. coli* and *S.aureus* in nutrient containing PBS in the present of the selected particles. Initial bacteria concentration is 4×10^7 CFU/mL.

biofilm, anti-QS and antibacterial properties of its VPBA and DMA contents. Although DMA containing particles shows anti-QS capability, quaternized DMA-containing particles did not showed it.[41] Owing to these properties, the PVBC-*g*-P8QDMA SPB can partially stop the reproduction of the bacteria so that antibacterial surface can be available after cleaning the dead bacteria from the surface.

On the other hand, inhibition effect of PVBC-*g*-P(VPBA-*b*-DMA) SPB that possesses less antibacterial and anti-QS activity, on *S. aureus* growth was found as weaker than PVBC-*g*-P8QDMA (Figure 7(b)). Additionally, Table 1 also shows that these two SPBs have the highest antibacterial effect in nutrient-containing PBS against *S. aureus*.

PVBC-*g*-P(VPBA-*b*-8QDMA) SPB (Figure 7) provided least antibacterial activities against both bacteria in the nutrient containing PBS, similar to the results obtained in the medium containing nutrients (Table 1). In the absence of nutrients, better antibacterial results were obtained because of no bacterial replication occurs (Figure 6). In this environment, quaternized nitrogens directly kills the bacteria, thus anti-QS property is not required. In this case, the high antibacterial activities of the P8QDMA segments in PVBC-*g*-P(VPBA-*b*-8QDMA) SPB is more pronounced as compared with the PVBC-*g*-P(VPBA-*b*-DMA) SPB that carries anti-QS properties.

Evaluation of these results suggests that if the nutrients are present in the medium, it will effectively prevent the bacterial reproduction with microbeads carrying anti-biofilm and anti-QS properties. However, in nutrient-free environments, since anti-QS is insignificant, microbeads with only bactericidal groups are more effective antibacterials.

3.3. Repeatability of antibacterial activity

The antibacterial activity of PVBC-*g*-P(VPBA-*co*-DMA), PVBC-*g*-P(VPBA-*co*-8QDMA), and PVBC-*g*-P8QDMA slightly decreased after repeated uses. PVBC-*g*-P(VPBA-*co*-8QDMA), on the other hand, reflected less activity reduction as compared to others.

ATR-FTIR results of SPBs after 3rd and 10th consecutive use against both bacteria are given in Figure 8. Since the results of SPBs were almost similar after 3rd use against both bacteria, only one spectrum is given in Figure 8(a-i, b-i, and c-i). The bands appeared at ~3300 (stretching; -NH_2, >NH and -OH), ~2960 (stretching; C-H), ~1600 (bending; -NH_2 and stretching; C=O, C=N), ~1400 (bending and stretch; aliphatic), and ~1100 (asymmetric stretching; C=O, P=O, P-O-C, P-O-P) confirms the adherence of *E. coli* and *S. aureus* on particle surface.[54,55] Although there is a substantial change in the intensity of these peaks for PVBC-*g*-P8QDMA SPB (Figure 8(b-ii and b-iii)), the change is very slight in case of PVBC-*g*-P(VPBA-*b*-DMA) SPB against *E.coli* (Figure 8(a-ii)) and negligible against both bacteria with PVBC-*g*-P(VPBA-*b*-8QDMA) SPB (Figure 8(c-ii and c-iii)) usage.

After 10th usage, the SEM photographs of PVBC-*g*-P(VPBA-*b*-DMA) and PVBC-*g*-P8QDMA SPBs before and after interaction with *E. coli* and *S. aureus* were obtained and are given in Figure 9. It can be seen that *S. aureus* are embedded on the PVBC-*g*-P8QDMA SPB surface (Figure 9(c)), while few on the surface of PVBC-*g*-P(VPBA-*b*-DMA) SPB (Figure 9(a) and (b)). These images support the idea that PVPBA has a repulsive effect against the

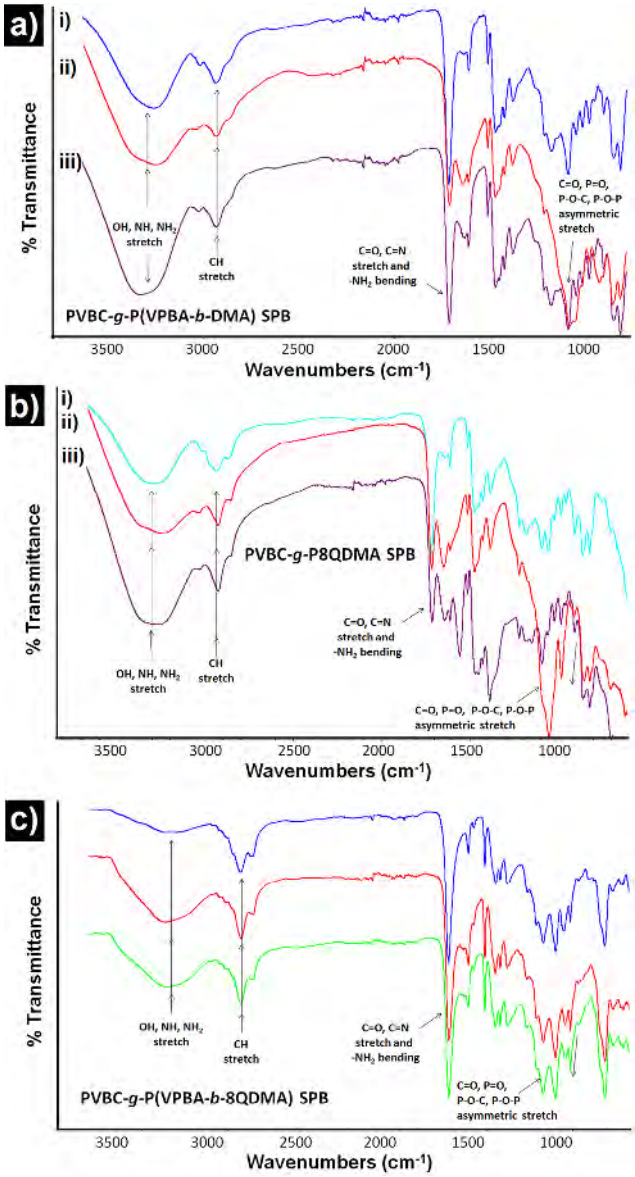

Figure 8. ATR-FTIR spectra of various microbeads after use in the antibacterial tests; (a) PVBC-*g*-P(VPBA-*b*-DMA) SPB, (b) PVBC-*g*-P8QDMA SPB, and (c) PVBC-*g*-P(VPBA-*b*-8QDMA) SPB ((i) *E. coli* and *S.aureus* after 3th, (ii) *E. coli* 10th and (iii) *S.aureus* 10th usage).

bacteria. The surface image after purifying PVBC-*g*-P(VPBA-*b*-DMA) SPB (Figure 9(d)) after interaction with the *E. coli* is very close to the original surface (Figure 9(g)). However, the purified surface (Figure 9(e)) in case of *S. aureus* appears to have less pores than the original surface (Figure 9(g)). The results support our interpretations that the PVPBA chains against *S.aureus* are less effective. For the PVBC-*g*-P8QDMA SPB, it is clear from the pores that the purified surface (Figure 9(f)) after interaction with *S. aureus* greatly differs from the original surface (Figure 9(h)). The results also supports the interpretations of ATR-FTIR spectra of PVBC-*g*-P(VPBA-*b*-8QDMA) SPB containing PVPBA as expressed in Figure 8(c-iii).

Although PVBC-*g*-P(VPBA-*b*-DMA) and especially PVBC-*g*-P(VPBA-*b*-8QDMA) SPBs can be used repeatedly after purification with proposed method, PVBC-*g*-P8QDMA SPB may not be recycled for antibacterial activity that is against the reported findings.[2,56] These results suggest that PVBC-*g*-P(VPBA-*b*-8QDMA) SPB may be more suitable for long-term use and reproducible results, although they show somewhat lower antibacterial activity as compared to PVBC-*g*-P8QDMA SPB.

4. Conclusions

The main objective of this study is to obtain polymeric brushes with antibacterial effect in nutrient and nutrient free medium. For this purpose, PVBC microbeads were synthesized in different constructs containing DMA and VPBA copolymeric structures. One or more repeated antibacterial activities of these SPBs were tested against *E. coli* and *S. aureus* bacteria in the indicated media. Effective antibacterial activity against both bacteria were obtained with PVBC-*g*-P(VPBA-*b*-DMA) SPB in the medium containing nutrient due to its antibacterial, anti-biofilm and anti-QS properties. In addition, antibacterial kinetic studies of selected particles were performed in nutrient free phosphate buffer and bacterial growth reduction capability of particles were observed in the order of PVBC-*g*-P8QDMA>PVBC-*g*-P(VPBA-*b*-8QDMA)>PVBC-*g*-P(VPBA-*b*-DMA) for *E. coli and S. aureus*. Growth kinetic studies of selected SPBs in phosphate buffer containing nutrient revealed that PVBC-*g*-P8QDMA had an inhibition effect on the growth against *S.aureus* in particular. In nutrients contain-

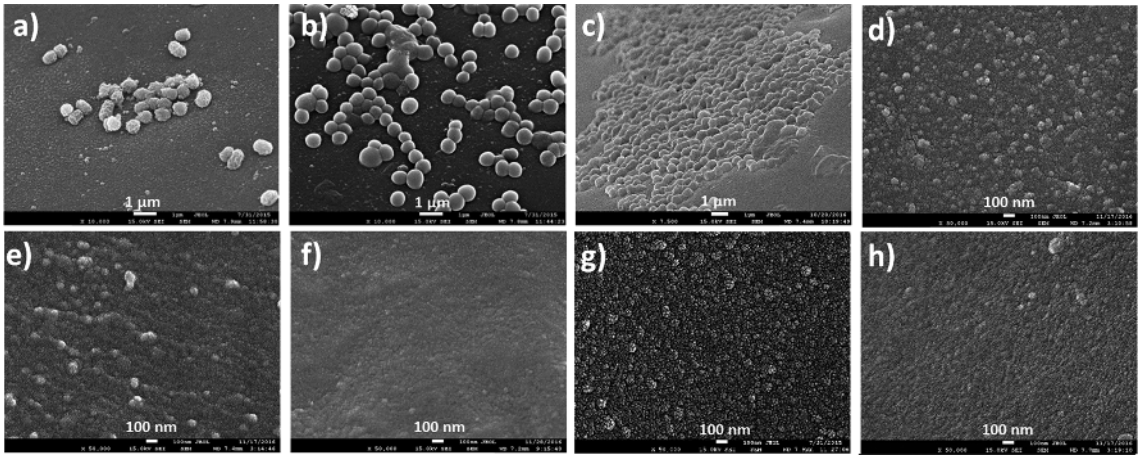

Figure 9. SEM images of particle surfaces after interactions with bacteria; (a) PVBC-*g*-P(VPBA-*b*-DMA) with *E.coli*, (b) PVBC-*g*-P(VPBA-*b*-DMA) with *S. aureus*, (c) PVBC-*g*-P8QDMA with *S. aureus* before purifying; cleaned forms are: (d) PVBC-*g*-P(VPBA-*b*-DMA), (e) PVBC-*g*-P(VPBA-*b*-DMA), (f) PVBC-*g*-P8QDMA; original surfaces: (g) PVBC-*g*-P(VPBA-*co*-DMA), (h) PVBC-*g*-P8QDMA.

ing medium, antibacterial, anti-QS and anti-biofilm properties gain importance. It was observed that the antibacterial effects of the SPBs obtained in the study continued with a decrease after reuse. The SPB having the best antibacterial effect was PVBC-*g*-P(VPBA-*co*-8QDMA). The continuity of antibacterial and anti-biofilm effects after re-use of SBPs and their interaction against bacteria have been successfully demonstrated by ATR-FTIR spectra and SEM images. As can be seen from the ATR-FTIR spectra, SPBs continue their antibacterial effect even though they are decreased against both bacteria even after the 3rd and 10th use. PVBPA chains have been shown to exert a repellent effect against *E. coli.* It has also been found that PVBC-*g*-P(VPBA-*b*-8QDMA) SPB may be more suitable for long-term use and reproducibility. By considering all results, the PVBC-*g*-P(VPBA-*b*-8QDMA) SPB has advantageous over PVBC-*g*-P8QDMA SPB for long-term and repeated applications. PVBC-*g*-P(VPBA-*b*-8QDMA) SPB has good potentials for wastewater treatment in fluidized bed reactors due to their long-lasting surface properties.

Supporting Information: Information is available regarding the experimental procedure for the preparation of different type of SPBs and their ATR-FTIR spectra. The materials are available *via* the Internet at http://www.springer.com/13233.

References

(1) S. K. Singh, J. Anamika, S. Dipak, and D. Arti, *Der Chemica Sinica*, **2**, 111 (2011).
(2) Z. P. Cheng, X. L. Zhu, Z. L. Shi, K. G. Neoh, and E. T. Kang, *Ind. Eng. Chem. Res.*, **44**, 7098 (2005).
(3) Z. P. Cheng, X. L. Zhu, Z. L. Shi, K. G. Neoh, and E. T. Kang, *Surf. Rev. Lett.*, **13**, 313 (2006).
(4) M. Z. Elsabee and E. S. Abdou, *Mater. Sci. Eng. C-Mater.*, **33**, 1819 (2013).
(5) Y. Liu, Y. Liu, X. H. Ren, and T. S. Huang, *Appl. Surf. Sci.*, **296**, 231 (2014).
(6) H. P. Yu, Y. C. Fu, G. Li, and Y. X. Liu, *Holzforschung*, **67**, 455 (2013).
(7) D. Roy, J. S. Knapp, J. T. Guthrie, and S. Perrier, *Biomacromolecules*, **9**, 91 (2008).
(8) F. Tang, L. F. Zhang, Z. B. Zhang, Z. P. Cheng, and X. L. Zhu, *J. Macromol. Sci. A*, **46**, 989 (2009).
(9) P. Limpiteeprakan and S. Babel, *Environ. Monit. Assess*, **188** (2016).
(10) F. Siedenbiedel and J. C. Tiller, *Polymers*, **4**, 46 (2012).
(11) L. L. Maharaj, M. M. Gupta, and A. K. Gadad, *World J. Pharm. Pharm. Sci.*, **4**, 126 (2015).
(12) S. Edmondson and S. P. Armes, *Polym. Int.*, **58**, 307 (2009).
(13) V. Mittal, *Polymers*, **2**, 40 (2010).
(14) H. Suzuki, M. Murou, H. Kitano, K. Ohno, and Y. Saruwatari, *Colloids Surf. B: Biointerfaces*, **84**, 111 (2011).
(15) F. J. Xu, S. J. Yuan, S. O. Pehkonen, E. T. Kang, and K. G. Neoh, *NanoBiotechnology*, **2**, 123 (2006).
(16) A. Khabibullin, E. Mastan, K. Matyjaszewski, and S. P. Zhu, in *Controlled Radical Polymerization at and from Solid Surfaces*, P. Vana, Ed. 2016, Vol. 270, pp 29-76.
(17) C. J. Fristrup, K. Jankova, and S. Hvilsted, *Soft Matter*, **5**, 4623 (2009).
(18) B. W. Brooks, *Chem. Eng. Technol.*, **33**, 1737 (2010).
(19) M. Charnley, M. Textor, and C. Acikgoz, *React. Funct. Polym.*, **71**, 329 (2011).
(20) M. T. Gokmen and F. E. Du Prez, *Prog. Polym. Sci.*, **37**, 365 (2012).
(21) F. X. Hu, K. G. Neoh, L. Cen, and E. T. Kang, *Biotechnol. Bioeng.*, **89**, 474 (2005).
(22) A. J. Kugel, S. M. Ebert, S. J. Stafslien, I. Hevus, A. Kohut, A. Voronov, and B. J. Chisholm, *React. Funct. Polym.*, **72**, 69 (2012).
(23) S. Senel, H. Cicek, and A. Tuncel, *J. Appl. Polym. Sci.*, **67**, 1319 (1998).
(24) S. Slomkowski and T. Basinska, *Macromol. Symp.*, **295**, 13 (2010).
(25) R. Tomovska, J. C. de la Cal, and J. M. Asua, in *Monitoring Polymerization Reactions*, John Wiley & Sons, 2013, pp 59-77.
(26) S. B. Lee, R. R. Koepsel, S. W. Morley, K. Matyjaszewski, Y. J. Sun, and A. J. Russell, *Biomacromolecules*, **5**, 877 (2004).
(27) G. Q. Lu, D. C. Wu, and R. W. Fu, *React. Funct. Polym.*, **67**, 355 (2007).
(28) H. Murata, R. R. Koepsel, K. Matyjaszewski, and A. J. Russell, *Biomaterials*, **28**, 4870 (2007).
(29) L. Timofeeva and N. Kleshcheva, *Appl. Microbiol. Biot.*, **89**, 475 (2011).
(30) F. Q. Zeng, Y. Q. Shen, S. P. Zhu, and R. Pelton, *J. Polym. Sci. Pol. Chem.*, **38**, 3821 (2000).
(31) S. J. Baker, C. Z. Ding, T. Akama, Y.-K. Zhang, V. Hernandez, and Y. Xia, *Future Medicinal Chemistry*, **1**, 1275 (2009).
(32) Y. J. Chang, X. Z. Liu, Q. Zhao, X. H. Yang, K. M. Wang, Q. Wang, M. Lin, and M. Yang, *Chinese Chem. Lett.*, **26**, 1203 (2015).
(33) B. Elmas, M. A. Onur, S. Senel, and A. Tuncel, *Colloid Polym. Sci.*, **280**, 1137 (2002).
(34) X. B. Li, J. Pennington, J. F. Stobaugh, and C. Schoneich, *Anal. Biochem.*, **372**, 227 (2008).
(35) Z. Lin, H. Huang, S. H. Li, J. Wang, X. Q. Tan, L. Zhang, and G. N. Chen, *J. Chromatogr. A*, **1271**, 115 (2013).
(36) S. Senel, *Colloid Surf. A*, **219**, 17 (2003).
(37) J. Zhang, Y. L. Ni, and X. L. Zheng, *J. Sep. Sci.*, **38**, 81 (2015).
(38) A. Adamczyk-Wozniak, O. Komarovska-Porokhnyavets, B. Misterkiewicz, V. P. Novikov, and A. Sporzynski, *Appl. Organomet. Chem.*, **26**, 390 (2012).
(39) N. T. Ni, H. T. Chou, J. F. Wang, M. Y. Li, C. D. Lu, P. C. Tai, and B. H. Wang, *Biochem. Biophys. Res. Commun.*, **369**, 590 (2008).
(40) G. Kocak, H. Cicek, Ö. Ceylan, and V. Bütün, *J. Appl. Polym. Sci.*, **136**, 46907 (2019).
(41) H. Cicek, G. Kocak, O. Ceylan, E. A. Kutluca, Z. Dikmen, and V. Butun, *J. Appl. Polym. Sci.*, **135**, 46245 (2018).
(42) E. Yavuz, G. Bayramoglu, B. F. Senkal, and M. Y. Arica, *J. Appl. Polym. Sci.*, **113**, 2661 (2009).
(43) Y. Man, G. Peng, X. F. Lv, Y. L. Liang, Y. Wang, Y. Chen, and Y. L. Deng, *Chromatographia*, **78**, 157 (2015).
(44) E. Yancheva, D. Paneva, V. Maximova, L. Mespouille, P. Dubois, N. Manolova, and I. Rashkov, *Biomacromolecules*, **8**, 976 (2007).
(45) B. Suart, *Infrared Spectroscopy: Fundamental and Applications*, John Wiley & Sons, Ltd, 2004.
(46) G. Kahraman, O. Beskardes, Z. M. O. Rzaev, and E. Piskin, *Polymer*, **45**, 5813 (2004).
(47) O. Cetinkaya, M. E. Duru, and H. Cicek, *J. Chromatogr. B*, **909**, 51 (2012).
(48) W. T. Lu, Z. G. Shao, G. Zhang, Y. Zhao, and B. L. Yi, *J. Power Sources*, **248**, 905 (2014).
(49) J. M. Song, S. Y. Lee, H. S. Woo, J. Y. Sohn, and J. Shin, *J. Polym. Sci. Pol. Phys.*, **52**, 517 (2014).
(50) M. Karamitrou, E. Sarpaki, and G. Bokias, *J. Appl. Polym. Sci.*, **133** (2016).
(51) D. Roy, J. T. Guthrie, and S. Perrier, *Soft Matter*, **4**, 145 (2008).
(52) M. Wiacek, D. Wesolek, S. Rojewski, K. Bujnowicz, and E. Schab-Balcerzak, *Polym. Adv. Technol.*, **26**, 49 (2015).
(53) A. King, S. Chakrabarty, W. Zhang, X. M. Zeng, D. E. Ohman, L. F. Wood, S. Abraham, R. Rao, and K. J. Wynne, *Biomacromolecules*, **15**, 456 (2014).
(54) Z. Filip, S. Hermann, and K. Demnerova, *Czech J. Food Sci.*, **26**, 458 (2008).
(55) L. D'Souza, P. Devi, T. Kamat, and C. G. Naik, *Indian J. Mar. Sci.*, **38**, 45 (2009).
(56) M. Ashfaq, S. Khan, and N. Verma, *Biochem. Eng. J.*, **90**, 79 (2014).